Secreted Frizzled-related Protein 3 (sFRP3)-mediated suppression of Interleukin-6 receptor release by A disintegrin and metalloprotease 17 (ADAM17) is abrogated in the osteoarthritis-associated rare double variant of sFRP3

Mirja Oldefest*, Stefan Düsterhöft*, Christine Desel*, Sarah Thysen†, Christine Fink‡, Björn Rabe*, Rik Lories†, Joachim Grötzinger*, Inken Lorenzen*[1]

*Institute of Biochemistry, Christian-Albrechts-University, Olshausenstr. 40, 24098 Kiel, Germany.

†Laboratory of Tissue Homeostasis and Disease, Skeletal Biology and Engineering Research Center, Department of Development and Regeneration, KU Leuven, Herestraat 49, 3000 Leuven, Belgium.

‡Institute of Zoology, Molecular Physiology, Christian-Albrechts-University, Am Botanischen Garten 3-9, 24118 Kiel, Germany.

[1]To whom correspondence should be addressed (email: ilorenzen@biochem.uni-kiel.de)

ABSTRACT

To avoid malformation and disease, tissue development and homeostasis are coordinated precisely in time and space. Secreted Frizzled-related protein 3 (sFRP3), encoded by the Frizzled-related protein gene (*FRZB*), acts as an antagonist of Wnt signalling in bone development by delaying the maturation of proliferative chondrocytes into hypertrophic chondrocytes. A disintegrin and metalloprotease 17 (ADAM17) is a transmembrane protease that is essential for developmental processes and promotes cartilage maturation into bone. sFRP3 is chondroprotective and is expressed in chondrocytes of healthy articular cartilage. Upon damage to cartilage, sFRP3 is down-regulated. Rare variants of sFRP3 are associated with osteoarthritis. This study demonstrates a novel function of sFRP3 in suppression of the enzymatic activity of ADAM17 which results in the inhibition of ADAM17-meditated interleukin-6 receptor (IL-6R) shedding. By contrast, the rare double variant of sFRP3 failed to suppress ADAM17. The shed soluble IL-6R is linked to inflammation, cartilage degeneration, and osteolysis. Accordingly, enhanced activity of ADAM17 in cartilage, caused by the expression of the rare double sFRP3 variant, provides an explanation for the genetic effect of sFRP3 variants in joint disease. The finding that sFRP3 interacts with the ADAM17 substrate IL-6R also suggests a new regulatory mechanism by which the substrate is protected against shedding.

Key words: ADAM17, sFRPs, FRZB, Osteoarthritis, metalloprotease, IL-6R, ectodomain shedding, SNPs.

Summary Statement: ADAM17 activity and sFRP3 down-regulation or expression of its rare double variant is associated with arthritis. sFRP3 interacts with IL-6R and ADAM17 and suppresses ADAM17 activity, whereas the rare variant doesn't; these findings provide explanation for their opposing pathogenic associations.

Short title: A rare variant of sFRP3 failed to suppress ADAM17

INTRODUCTION

Tissue development and homeostasis are highly complex processes that are tightly controlled in time and space. Secreted Frizzled-related protein 3 (sFRP3), encoded by the Frizzled-related protein gene (*FRZB*), was identified in a chondrogenic extract of articular cartilage during a search for proteins critical for bone development, and is expressed by chondrocytes in developing bone and articular cartilage [1-4]. During long bone development, pre-chondrogenic cells mature into proliferating chondrocytes, which secrete components of the extracellular matrix, resulting in growth of the cartilaginous bone template. Later, these cells differentiate into hypertrophic cells that mineralize the surrounding cartilage. sFRP3 suppresses this differentiation into hypertrophic chondrocytes; thus sFRP3 expression is deliberately reduced during this developmental stage [3]. By contrast, chondrocytes in articular cartilage, which continually express sFRP3, show no differentiation into hypertrophy.

Evidence shows that sFRP3 plays a significant role in bone development and cartilage homeostasis. Overexpression of sFRP3 in developing chicken limbs leads to shortening of long bones and joint fusion, a phenotype that is associated with a delayed maturation of hypertrophic chondrocytes [3]. In addition, sFRP3 knock-out mice show enhanced articular cartilage loss in osteoarthritis disease models [5]. Two single nucleotide polymorphisms in the gene encoding sFRP3, which lead to amino acid changes R200W and R324G, are linked to osteoarthritis and other skeletal diseases [6-10], as well as cancer progression [11, 12].

sFRP3 belongs to the mammalian sFRP family, which comprises five well-established Wnt antagonists (sFRP1-5) [13]; hence the biological effects of sFRP3 have been connected primarily to its role in Wnt signalling [14-19]. All sFRPs consist of an N-terminal cysteine-rich domain (CRD) and a C-terminal Netrin (Ntr)-like domain. The CRD is homologous to those of Frizzled receptors and represents the classical binding module of Wnt proteins [20]. Similar to those of Frizzled receptors, the CRDs of sFRPs bind to Wnt proteins and the CRD of sFRP3 antagonizes Wnt signalling in an identical manner to the full-length protein [21].

Whereas the CRDs of sFRPs are well characterized, little is known about the Ntr-like domains, which are thought to act as heparin- and heparan sulphate-binding modules [22-25]; however, additional functions have also been proposed. For instance, the Ntr-like domain of sFRP1 binds to the N-terminal module of thrombospondin-1, thereby inhibiting its interaction with $\alpha_3\beta_1$ integrin and preventing cell adhesion [26]. In addition to those in sFRPs, C-terminal Ntr-like domains are also present in proteins such as netrin-1, procollagen peptidase enhancer 1, and the complement factors C3, C4, and C5 [27]. N-terminal Ntr-like domains are present in tissue inhibitors of metalloproteases (TIMPs) [27]. Intriguingly, members of the sFRP family act as inhibitors of metalloproteases belonging to the metzincin family, including matrix metalloproteases (MMPs), A disintegrin and metalloproteases (ADAMs) and A disintegrin-like and metalloprotease with thrombospondin type 1 repeats (ADAMTS) [28]. The sFRPs Sizzled and Crescent are not thought to play a role in Wnt binding, but are well-described inhibitors of tolloid-like metalloproteases, such as bone morphogenetic protein 1 [29-32]. Furthermore, sFRP3 suppress MMP2 activity in prostate cancer cells [33] and interacts directly with MMP3, whereupon its enzymatic activity is reduced [5]. sFRP1 suppresses ADAM10 activity, which is also most likely due to a direct protein-protein interaction [34].

ADAM10 is the closest relative of ADAM17, which is required for proper long bone development [35, 36]. ADAM17, a transmembrane type-I metalloprotease, was initially shown to cleave membrane-bound tumour necrosis factor α (TNFα), resulting in the release of the actual pro-inflammatory active cytokine [37, 38]. ADAM17 can also cleave cytokine receptors such as the interleukin-6 receptor (IL-6R), and membrane-bound proforms of epidermal growth factor receptor ligands, such as transforming growth factor α (TGFα). The release of these substrates from the cell surface is called shedding [39]. These substrates imply the role for ADAM17 in developmental processes; accordingly, ADAM17 null mice display perinatal lethality [40].

Selective deletion of ADAM17 in mouse chondrocytes demonstrates its importance in bone development [35, 36]; compared with wild type animals, these mice display shorter long bones with extended hypertrophic zones. This growth retardation is the consequence of delayed remodelling of the hypertrophic cartilage template to bone caused by a halt in differentiation, most likely due to the absence of TGFα release by ADAM17 [35, 36]. This phenotype is similar to that of chicken embryos overexpressing sFRP3 [3]. IL-6R is another prominent substrate of ADAM17, and is connected to bone homeostasis. Similar to the membrane-bound proform of TNFα, membrane-bound IL-6R is associated with regenerative processes and only becomes a pro-inflammatory mediator after shedding from the cell surface [39, 41, 42]. The shed soluble IL-6R (sIL-6R) promotes pathological inflammatory responses [42-44], but also induces osteolytic conditions due to its positive effect on osteoclastogenesis [45, 46]. Activation of chondrocytes by the IL-6/IL-6R complex stimulates expression of the aggrecanases ADAMTS4 and ADAMTS5, which promote cartilage degeneration [47].

ADAM17 can act as a releasing factor of TNFα and sIL-6R in the synovial fluids of arthritis patients, and the amount of sIL-6R in the synovial fluid correlates with the grade of joint destruction [41, 48]. The aim of this study was to unravel the relationships between the chondroprotective sFRP3 and ADAM17, and the joint destructive sIL-6R. sFRP3 suppressed ADAM17, thereby preventing sIL-6R release. The rare sFRP3 double variant was not able to perform this task, which might be an explanation for its association with joint degenerative diseases.

EXPERIMENTAL

sFRP3 expression constructs

For easy detection of sFRP3, a PC-tag was introduced between its signal peptide and its CRD. This cDNA was obtained from Life Technologies/GeneArt (Regensburg, Germany) and cloned into pcDNA3.1 (-) via NheI and NotI cleavage sites.
The amino acid exchanges of the rare variants were introduced by site directed mutagenesis. To introduce the R200W exchange, an overlapping PCR was applied, using primer pair, forward and part1_rev, as well as, part2_fwd and reverse, or rev_R324G. The latter pair (part2_fwd and rev_R324G) was used to obtain the rare double variant. To obtain the single R324G variant, the primer pair forward and rev_R324G was used.

primer	mutation	sequence
forward	R200W;R324G	GCAGCTAGCGCCACCATGGTCTGCGGC
part1_rev	R200W	AGTCTTTATCTCTTTAACTTTAGCCCAAATGACATAGTTGTAATTGTTCCG
part2_fwd	R200W	TACAACTATGTCATTTGGGCTAAAGTTAAAGAGATAAAGACTAAGTGC
rev_R324G	R324G	TTTTCCTTTTGCGGCCGCTTAGTTGCCTGCTTGCCGGGGGTTCG
reverse	R200W	TTTTCCTTTTGCGGCCGCTTAGTTGCGTGCTTGCCGGGGGTTCG

Cell culture and transfection

HEK293T cells and PC3 cell lines were cultured in a humidified incubator at 37 °C, 5 % CO_2, in Dulbecco's modified Eagle's medium (DMEM) high-glucose with 10 % foetal calf serum (FCS), streptomycin (100 mg/l) and penicillin (60 mg/l) (all from PAA Laboratories, Cölbe, Germany).
For pull-down and co-immunoprecipitation experiments, 2×10^6 HEK293T cells were seeded in 10 cm culture dishes. After 24 h, a pre-mixed solution of 8 µg DNA and 20 µl polyethylenimine (1 mg/ml) in 1 ml DMEM was added for transient transfection. Cells were harvested 48 h after transfection.
For flow cytometric analysis, immunofluorescence staining, proximity ligation assay - and ADAM17 activity assays, cells were transfected using a mixture of 2 µg DNA and 5 µl polyethylenimine (1 mg/ml) in 100 µl DMEM. 0.3×10^6 HEK293T cells were seeded 1 day prior to transfection for immunofluorescence- and proximity ligation assay. 0.45×10^6 cells were seeded 1 day prior to transfection for flow cytometric analysis and ADAM17 activity assay.

ADAM17 activity assay

ADAM17 endogenously expressing HEK293T cells were used to measure shedding activity of ADAM17, by co-transfecting them with extracellularly alkaline phosphatase (AP)-tagged substrates (IL-6R, proTNFα or proTGFα) [49] and sFRP3 variants or empty vector. One day later, cells were stimulated; for that medium was replaced by DMEM plus 100 µM cycloheximide (Sigma-Aldrich, Taufkirchen, Germany) supplemented either with dimethylsulfoxide (DMSO), 100 nM phorbol-12-myristate-13-acetate (PMA) [50, 51] (Sigma-Aldrich, Taufkirchen, Germany) or 100 nM PMA plus 10 µM of the metalloprotease inhibitor marimastat (Merck, Darmstadt, Germany). After 30 minutes (in case of TNFα one hour), supernatants and cells were harvested, AP activities were measured and the relative shedding activities were calculated as described

previously [49, 51, 52]. In brief, cells were lysed in lysis buffer (50 mM Tris (pH 7.5), 200 mM NaCl, 2 mM EDTA, 1 % Triton X-100 and complete protease inhibitor mixture without EDTA (Roche Applied Science, Mannheim, Germany)). AP activities of supernatants and cell lysates were measured at 405 nm using p-nitrophenylphosphate (Sigma-Aldrich, Taufkirchen, Germany) as substrate. Absorptions of supernatants were divided by those of the corresponding lysates. The obtained ratios were normalized to the corresponding sample treated with metalloprotease inhibitor marimastat and PMA which were set to one. Afterwards, the shedding activity of the PMA-treated control sample was set to 100 %. Student's *t*-tests were performed using the online tool at http://www.physics.csbsju.edu/stats/t-test.html.
Conditioned media was obtained from HEK293T cells cultured in DMEM containing 5 % FCS which were transfected with eGFP as control or indicated variants of sFRP3. After two days supernatants were harvested, sterile filtered and frozen at –20 °C. Expression of sFRP3 constructs was proven by Western blot analysis of aliquots from the supernatant. After expression of the constructs of interest was confirmed, the conditioned media was diluted one to one and applied in the activity assay using HEK293T cells solely transfected with AP-tagged IL-6R, in the same way as described for DMEM medium with cycloheximide.

Western blotting

To confirm successful expression of proteins of interest, Western blot analysis was performed as described previously [53]. For detection of PC-tagged sFRP3 variants murine HPC4 antibody (Ab) was applied in the presence of 4 mM $CaCl_2$ in the antibody- and washing buffers. Expression of ADAM17 was detected using A300D monoclonal antibody (mAb) [54], expression of the IL-6R was detected with the murine 4-11 Ab [55], and β-actin expression was detected using C4 mAb (Santa Cruz Biotechnologies, USA). AP-tagged proTNFα was detected via its myc-tag (71D10 Cell Signaling, USA) and AP-tagged proTGFα via its AP-tag (ab11299, Abcam, England).

Wnt Signalling Phospho Antibody Microarray.

Two samples were analysed with the Wnt Signaling Phospho Antibody Microarray (Full moon BioSystems/ Bio Cat, Heidelberg, Germany). To obtain them an ADAM17 activity assay was performed by applying conditioned media containing 100 nM PMA on HEK293T cells. One sample was treated with conditioned medium from sFRP3 transfected HEK293T cells, the second one was treated with conditioned medium from eGFP transfected HEK293T cells. Five minutes after stimulation cells were harvested and subjected to the Wnt Signalling Phospho Antibody Microarray, which was performed according to manufacturer's instructions. This assay was performed once only as no changes were observed in the Wnt pathway.

Co-immunoprecipitation experiments

Co-immunoprecipitation experiments were performed as described previously [56]. "Lysis buffer plus sucrose" (50 mM Tris (pH 7.5), 200 mM NaCl, 2 mM EDTA, 0.5 % Triton X-100, 5 % glycerol, 250 mM sucrose, complete protease inhibitor mixture without EDTA (Roche Applied Science, Mannheim, Germany) and marimastat (Merck, Darmstadt, Germany, 10 µM) were used. In brief, beads were pre-incubated with lysis buffer supplemented with 6 % BSA. HA-tagged ADAM17 was immunoprecipitated using rabbit anti-HA Ab (C29F4, Cell Signaling, USA) and Protein A beads (Thermo Scientific, USA). To precipitate wild type ADAM17 A300E mAb [57,

58] and Protein G (Thermo Scientific, USA) beads were applied. Cell lysates were divided into two aliquots, after an input sample was taken. In one aliquot Abs and beads were added. In the second aliquot, only beads were added, to serve as control. After incubation, beads were washed and analysed by Western blotting. Experiments were performed and thereby reproduced in at least 3 independent experiments.

Flow cytometric analysis

Flow cytometric analysis was performed as described previously [53]. PC3 cells were stimulated, 5 minutes prior to staining, by the addition of 100 nM PMA. Afterwards, 3×10^5 PC3 cells or 5×10^5 HEK293T cells were washed twice in FACS solution (PBS, 0.05 % NaN_3) and stained for 1 h at 4 °C with 20–30 µg/ml of primary Abs. For detection of ADAM17, anti-ADAM17 A300E mAb [54], for the IL-6R, murine anti-IL-6R 4-11 mAb [55], and for detection of PC-tagged sFRP3 constructs, murine HPC4 mAb was used. When using HPC4, PBS was replaced by HEPES buffer (10 mM HEPES (pH 7.5), 140 mM NaCl, 4 mM KCl, 0.75 mM $MgCl_2$, 3 mM $CaCl_2$). Afterwards, cells were washed and stained with 2 µl of allophycocyanin-conjugated goat anti-mouse IgG (Jackson ImmunoResearch Laboratories, USA) for 1 h at 4 °C. Subsequently, cells were measured with a FACScan flow cytometer (BD Biosciences; USA) and experiments were analysed using BD FACSDiva software. All presented flow cytometric measurements were confirmed at least 3 times in independent experiments.

Co-immunostaining experiments

HEK293T cells (0.3×10^6) were seeded in six-well plates on coverslips one day prior to transfection. Two days after transfection, cells were used for co-immunostaining experiments. In the case of PMA stimulation, 100 nM PMA was added for 5 minutes. Afterwards, coverslips were washed with PBS, blocked with 10 % FCS and incubated sequentially for 1–2 h with primary and secondary Abs at 4 °C. Cells were then fixed by incubation with 4 % paraformaldehyde (Merck, Darmstadt, Germany) at room temperature, the reaction was stopped by incubation with 0.12 % glycine in PBS, followed by the addition of Mowiol 4-88 (151 mg/ml Calbiochem, USA)/ Diazabicyclooctan (18 mg/ml, Sigma-Aldrich, Taufkirchen, Germany) plus DAPI in PBS for anchorage onto object plate. Objects were analysed by confocal fluorescence microscopy (Olympus IX 81, cLSM FluoView 1000, Olympus, Hamburg, Germany). For staining of ADAM17 murine A300E mAb, for sFRP3 rabbit H170 Ab (Santa Cruz Biotechnologies, USA) and for staining of IL-6R murine 4-11 mAb was used. The following secondary tools were used for detection: Alexa Fluor® 488 Goat Anti-Rabbit Ab (A11034) and Alexa Fluor® 594 Goat Anti-Mouse Ab (A11032; both from Life Technologies, Regensburg, Germany).

Proximity ligation assay

The *Duolink in Situ® Assay* (Sigma-Aldrich, Germany) was used to perform proximity ligation assays. Cells were seeded and treated as for co-immunostaining experiments. The assays were performed according to manufacturer's instructions. For primary Abs, the same Abs were used as in the co-immunostaining experiments, presenting a pair of murine and rabbit primary Abs. The co-immunostaining experiments proximity ligation assays were repeated and confirmed in 3 independent experiments.

Surface biotinylation assay

For biotinylation of cell surface proteins HEK293T cells were washed 3 times with PBS (pH 7.4), ones with PBS (pH 8, 4 °C), incubated with 5 ml of 0.25 mg/ml EZ-Link Sulfo-NHS-LC-Biotin (Perbio Science, Germany) in PBS (pH 8) for 45 minutes at 4 °C and afterwards harvested.
Harvested cells were lysed in lysis buffer (20 mM Tris (pH 7.4), 150 mM NaCl, 2 mM EDTA, 0.5 % Triton X-100, 0.1 % SDS and complete protease inhibitor mixture without EDTA (Roche Applied Science, Germany)). Protein concentration was measured using the BCA Protein Assay Kit (Perbio Science, Germany). For pull-down of biotinylated proteins 2000 µg were incubated with 40 µl streptavidin beads for 1 h at 4 °C. Afterwards beads were washed three times with lysis buffer and three times with wash buffer (20 mM Tris (pH 7.4), 500 mM NaCl, 2 mM EDTA, 0.5 % Triton X-100). For Western Blot analysis the beads were heated in 70 µl 2.5x Lämmli buffer.

Surface plasmon resonance measurement

Affinity measurements were performed using a BiacoreX100 (GE Healthcare, Germany). Recombinant ectodomain of the human ADAM17 (R&D systems; 930-ADB-010/CF) in a 1:1 mixture of PBS (pH 7.4) and 10 mM acetate buffer (pH 4) was immobilized on a CM5 biosensor chip (GE Healthcare, Germany) according to the manual. Recombinant human sFRP-3 (R&D systems; 192-SF-010/CF) was analysed in a range from 0.29 to 2.85 µM using PBS (pH 7.4) as running buffer.

RESULTS

ADAM17-mediated IL-6R shedding is suppressed by sFRP3

Because of the opposing roles of sFRP3 and ADAM17 in bone development and cartilage homeostasis, and the fact that sFRP1 suppresses ADAM10 activity [34], the influence of sFRP3 on ADAM17-mediated shedding was analysed (Figure 1A). HEK293T cells, which endogenously express ADAM17, were co-transfected with a plasmid encoding AP-tagged IL-6R, an ADAM17 substrate, and a plasmid encoding PC-tagged sFRP3 or empty vector as a control. At 1 day post-transfection, PMA was added to stimulate ADAM17 shedding activity [50, 51]. The AP activities in the supernatants and cell lysates were measured and used to calculate relative shedding activities. sFRP3 decreased ADAM17-dependent sIL-6R release (Figure 1A). A Western blot analysis of the cell lysates showed that this suppressive effect was not due to differences in the expression levels of the substrate, because the samples displayed comparable levels of IL-6R (Figure 1B).

Suppression of ADAM17-mediated IL-6R shedding is abrogated in the rare double sFRP3 variant

To examine the activities of sFRP3 variants, amino acid substitutions were introduced into the common variant and shedding assays were performed with the resulting rare single variant (R324G) and rare double variant (R200W R324G) (Figure 1A). In contrast to the single variant, the rare double sFRP3 variant failed to suppress ADAM17 activity, leading to an increased release of sIL-6R by ADAM17. A Western blot analysis showed that this effect was not due to differences in the expression levels of IL-6R or the sFRP3 variants (Figure 1B).

Since only the rare double variant of sFRP3, and not the single R324G variant, failed to suppress ADAM17-mediated IL-6R shedding, we investigated whether the failure of suppression was caused by the R200W exchange only, or whether both amino acid substitutions were required. For this experiment, the corresponding nucleotide was exchanged in the common sFRP3 variant and ADAM17 activity assays were performed. The R200W variant of sFRP3 showed the same inhibitory effect as the common variant, implying an additive effect of both amino acid substitutions in the rare double sFRP3 variant (Figure 1C).
To determine whether ADAM17 suppression is in fact mediated by secreted sFRP3, ADAM17 activity assays were performed in the presence of conditioned media. In the first series of experiments, these media were obtained from HEK293T cells expressing eGFP (as a control), sFRP3, the sFRP3 rare single variant (R324G), or the sFRP3 rare double variant (R200W R324G). The resulting data showed comparable effects to those observed in the previous activity assays. Since the data displayed high standard derivations, a second series of experiments were performed using new conditioned media, this time also from cells expressing the rare R200W variant. Both experimental runs confirmed the suppressive effect of sFRP3 on ADAM17 activity and its abrogation by the double variant but not the single variants of sFRP3 (Figures 1E and 1F).

Suppression of ADAM17 activity by sFRP3 does not have exclusive effects on the shedding of IL-6R

Besides IL-6R, ADAM17 also processes the membrane-bound proforms of TGFα and TNFα. Like sIL-6R, both of these soluble proteins are described in the context of cartilage and bone. Whereas TGFα is thought to be the key substrate of ADAM17 during bone development [35, 36], TNFα is a well-known mediator of inflammatory situations such as rheumatoid arthritis [41]; therefore, the suppressive effects of sFRP3 on ADAM17-mediated shedding of these two additional substrates were studied (Figures 1G and 1H). Notably, shedding of the proforms of TGFα and TNFα was reduced to approximately 30 % when sFRP3 was overexpressed, which was comparable to the effects of sFRP3 on the shedding of IL-6R.

Suppression of ADAM17 by sFRP3 is independent of Wnt signalling

sFRP3 is a well-known inhibitor of Wnt-mediated signalling; thus the involvement of Wnt signalling in sFRP3-mediated suppression of ADAM17 activity was investigated. HEK293T cells transfected with AP-tagged IL-6R were incubated with conditioned medium from sFRP3-transfected or eGFP-transfected HEK293T cells. After PMA stimulation for 5 minutes, the cells were harvested and activated/phosphorylated signalling molecules of the Wnt pathway were analysed using a Wnt Signaling Phospho Antibody Microarray. This array included probes for the β-catenin-dependent canonical pathway, the Wnt calcium pathway, and the Wnt planar cell polarity pathway. No differences between the phosphorylation levels of signalling molecules involved in the different Wnt Pathways were detected (Figures 2A–E). This result suggests that the suppressive effect of sFRP3 on ADAM17 activity is independent of its function as a Wnt antagonist. This hypothesis is reasonable because ADAM17 activity assays using transfected cells or conditioned media revealed the same suppressive effects, regardless of whether sFRP3 was present for a long time before stimulation or only a short time during stimulation.

ADAM17 and sFRP3 interact on the surface of cells

To determine whether the suppressive effect of sFRP3 on ADAM17 is mediated by a direct protein-protein interaction, as reported for sFRP1 and ADAM10 [34], co-immunoprecipitation experiments were performed. ADAM17 co-precipitated with sFRP3 after overexpression in HEK293T cells (Figure 3A). Next, lysates of untransfected HEK293T cells were used to determine whether these cells express sFRP3 endogenously. Subsequent co-precipitation experiments revealed an interaction between endogenously expressed sFRP3 and ADAM17 (Figure 3B).

A flow cytometry analysis was used to evaluate whether ADAM17 and sFRP3 interact on the cell surface. The human prostate cancer cell line PC3 was stably transfected with an ADAM17-specific shRNA to reduce ADAM17 expression, or a scrambled shRNA to ensure normal ADAM17 expression [59]. Western blot and flow cytometry analyses confirmed the successful suppression of ADAM17 expression in the PC3 knock-down cells (Figures 3C and 3D). The flow cytometric analysis also revealed that the amount of ADAM17 on the cell surface of both cell lines increased after 5 minutes of treatment with PMA. These cell lines were transiently transfected with N-terminal PC-tagged sFRP3 (Figure 4O) and treated with PMA for 5 minutes, at 1 day post-transfection. Afterwards, the localization of sFRP3 on the cell surface was determined by flow cytometry. Notably, the ADAM17-expressing control cells showed increased sFRP3 cell surface staining compared with the ADAM17 knock-down cells (Figure 3E).

To prove the interaction of sFRP3 and ADAM17 on the cell surface, co-immunostaining of non-permeabilized HEK293T cells was performed. Attempts to use endogenously expressed sFRP3 failed; therefore, HEK293T cells were transiently transfected with PC-tagged sFRP3. The transfected cells were stained with a murine A300E mAb, which detects the ectodomain of ADAM17, and a rabbit polyclonal anti-sFRP3 H170 Ab (Figures 4A–H). Overexpressed sFRP3 was clearly detectable on the surface of unstimulated HEK293T cells (Figure 4A). By contrast, there was very little ADAM17 staining on the surface of these cells (Figure 4B); however, the presence of ADAM17 on the cell surface increased upon PMA treatment (Figure 4F). In addition, in contrast to the untreated samples, the PMA-treated samples displayed colocalization of sFRP3 and ADAM17 of approximately 10 % (Figures 4C and 4D versus Figures 4G and 4H), indicating that these two proteins indeed interact on the cell surface. To confirm that the amount of ADAM17 on the surface of HEK293T cells increases upon stimulation with PMA, flow cytometric analyses and cell surface biotinylation experiments were performed (Figures 4I and 4J).

To strengthen the results indicating colocalization of ADAM17 and sFRP3 on the cell surface, proximity ligation assays were performed (Figures 4K and 4L). This highly sensitive method allows the detection of protein-protein interactions by fluorescent microscopy. Advantages of this method are that signals occur only in the case of close proximity of the target proteins, and the signals are amplified. Because of the high sensitivity of this method, endogenously expressed proteins were analysed. Also, HEK293T cells were stimulated for 5 minutes with PMA to increase the cell surface presence of ADAM17. The appearance of green spots (Figure 4K) indicated that endogenously expressed sFRP3 and ADAM17 interacted on the surface of HEK293T cells. To verify this direct interaction further, surface plasmon resonance measurements were performed with purified proteins (Figure 4M); these experiments revealed that the two proteins interacted directly, albeit with a low affinity (K_D ~1 μM).

The cell surface interaction with ADAM17 is abrogated by the rare double variant of sFRP3

The failure of the rare double sFRP3 variant to suppress ADAM17 could be due to a reduced interaction with the protein; hence, flow cytometric analyses of PC3 control cells and PC3 ADAM17 knock-down cells (Figures 3C and 3D) were performed with the sFRP3 variants (Figures 4N-4P). Both single variants, R200W and R324G, displayed an ADAM17-dependent cell surface association that was comparable to that of the common variant (Figure 3E). By contrast, the rare double variant did not exhibit this ADAM17-dependent cell surface association.

IL-6R interacts with sFRP3

Because sFRP3 suppresses the generation of sIL-6R, the question of whether sFRP3 binds to IL-6R, thereby preventing its release from the cell surface, was addressed. To this end, co-immunoprecipitation experiments were performed using lysates of co-transfected HEK293T cells expressing IL-6R and N-terminal PC-tagged sFRP3. Co-immunoprecipitation of PC-tagged sFRP3 with IL-6R was observed (Figure 5A) and *vice versa* (Figure 5B), providing evidence for an interaction between sFRP3 and IL-6R. To confirm this novel interaction, flow cytometry and proximity ligation assays were performed. For both types of experiments, HEK293T cells were transfected with IL-6R because they do not endogenously express this protein. For flow cytometry analyses, HEK293T cells were co-transfected with plasmids encoding sFRP3 and IL-6R, or a plasmid encoding sFRP3 or IL-6R and an empty vector as a control. These experiments revealed that the presence of IL-6R on the cell surface caused a significant increase in sFRP3 cell surface association (Figures 5C and 5D). This interaction was confirmed by a proximity ligation assay using a murine anti-IL-6R mAb [55] and a rabbit anti-sFRP3 Ab as primary Abs (Figures 5G and 5H). Because of differences between the expression levels of the endogenous and transfected proteins, it was not feasible to compare this result to that of the proximity ligation assays of the sFRP3-ADAM17 interaction.
This study shows that sFRP3 interacts specifically with ADAM17 and its substrate IL-6R, pointing to a new connection between a protease, a suppressor, and a substrate. By contrast, the rare double variant of sFRP3 failed to interact with ADAM17 and failed to suppress ADAM17-mediated IL-6R release. However, flow cytometry analyses showed that the rare double variant could still interact with IL-6R (Figures 5E and 5F). This result suggests that the rare double variant of sFRP3 lacks the cartilage protective effect because of its inability to interact with ADAM17.

DISCUSSION

sFRP3 is an antagonist of the Wnt signalling pathway and two rare coding variants of the secreted protein are associated with hip osteoarthritis. Notably, the amino acid substitutions in the rare sFRP3 variants are located within the C-terminal Ntr-like domain and not the N-terminal located CRD which is responsible for the Wnt antagonistic feature [21]. Although an effect on Wnt signalling was suggested in the original report [6], this link to the Ntr-like domain suggests a Wnt-independent association of the rare variants with osteoarthritis [6-10]. Western blot analyses of the common-, both single rare-, and the double rare variant of sFRP3 showed that all proteins were successfully expressed and properly secreted into the medium of transfected HEK293T cells (Figure 1F). The levels of secretion and expression of the rare variants appeared

to be comparable and were not lower than those of the common variant in our experimental setting. Thus, reduced levels of sFRP3 rare variants within the synovial fluid are unlikely, and the Wnt antagonistic capability would likely remain the same between variants.

Therefore, a Wnt signalling-independent function of sFRP3 that is dependent on its Ntr-like domain seems probable. Because overexpression of sFRP3 in chicken embryos causes a comparable phenotype [3] to the absence of ADAM17 in chondrocytes of mice [35, 36], namely shortened long bones, this protease seems to be an attractive candidate for suppression by sFRP3. Our *in vitro* studies confirmed this suppression of ADAM17 activity by sFRP3. By contrast, the rare double variant of sFRP3, which has reduced cartilage protective properties, failed to interact with ADAM17 or suppress its shedding activity towards IL-6R. These results suggest that the loss of cartilage protection observed for the rare double variant of sFRP3 might be due to an enhanced release of soluble factors into the synovial fluid by increased ADAM17 activity, caused by the inability of the rare double variant to interact and suppress the protease.

TIMPs are additional natural inhibitors of ADAM proteases that contain Ntr-like domains. TIMP3 inhibits the activity of ADAM17 [60]. In contrast to sFRPs, the Ntr-like domain of TIMPs is located at the N-terminus rather than the C-terminus. The N-termini of TIMPs are directly involved in inhibitory binding to the active centre of metalloproteases [61]; these interactions block the proteolytic activity of MMPs and ADAMs [61]. Because of differences in their domain structures, TIMPs and sFRPs do not suppress ADAMs in the same manner. Studies examining the well-established inhibitors of the sFRP family, Sizzled and Crescent, have reported that their inhibitory potential is dependent on the CRD, and not the Ntr-like domain [29-32]. However, the Ntr-like domain of sFRP3 has a major impact on the suppression of ADAM17, since two amino acid substitutions in this domain in the rare double variant lead to abrogation of ADAM17 binding and suppression. The specific interaction of sFRP3 with ADAM17 and the proper secretion of the rare double variant of sFRP3 indicates that the decreased cartilage degenerative potential of the rare variants, as well as the cell surface interaction of the common sFRP3 variant, are unlikely to be due to heparin/proteoglycan binding. The involvement of the Ntr-like domain in the interaction of sFRP3 with ADAM17 suggests that it is not limited to proteoglycan binding.

Soond *et al.* [62] demonstrated previously that ADAM17 is only prominently present on the cell surface upon its activation. Prior to its activation, the protease is located intracellularly in perinuclear regions. Also in the cell lines used here activation of ADAM17 leads to its translocation to the cell surface. Because only minor amounts of the enzyme were on the surface of non-stimulated cells no unambiguous statement can be made whether sFRP3 interacts with activated ADAM17 only, or whether this interaction also takes place in the secretory compartments prior to activation.

Because both sFRP3 and ADAM17 pass through the secretory pathway, it is difficult to use overexpression experiments to determine where they actually meet, since the densities of these proteins are extremely high in the endoplasmic reticulum and Golgi apparatus. Accordingly, the use of intracellular co-immunostaining to detect colocalization might be subject to concentration-dependent artefacts and may not reflect a specific interaction. Hence, it is a challenge for future research to clarify the timing and location of the initial sFRP3-ADAM17 interaction. The complexity of these molecular interactions is underlined further by the

observation that sFRP3 also interacts with IL-6R, a prominent substrate of ADAM17. The product of IL-6R shedding, sIL-6R, is involved in the degeneration of cartilage as well as bone [45-47]. The presence of the rare double variant of sFRP3 might result in an inadequate suppression of ADAM17 activity, thereby increasing the release of sIL-6R and promoting joint degeneration. The finding that sFRP3 interacts with both ADAM17 and IL-6R, leads to the fascinating idea that, upon activation and translocation of ADAM17 to the cell surface, the inhibitor is directly provided to the protease by the substrate. The low affinity interaction between sFRP3 and ADAM17 suggests that there might be cooperative binding, by which IL-6R increases the affinity of sFRP3 for ADAM17. This hypothesis suggests a new level of control, which could be necessary in systems or situations in which the activity of ADAM17, and therefore the release of factors from the cell surface, is particularly dangerous.

Since the rare double variant of sFRP3 failed to bind ADAM17 on the surface of cells but still bound to cell surface-located IL-6R, one might suggest that binding of ADAM17 by sFRP3 is essential for suppression of its enzymatic activity, particularly since the rare double variant failed to suppress IL-6R shedding by ADAM17. Additional work will be necessary to unravel the binding sites for sFRP3 within the protease and its substrate. These investigations will allow to determine whether sFRP3 blocks the binding or cleavage site in IL-6R, or whether its blocks the catalytic centre of ADAM17. Overexpression of sFRP3 leads to reduced release of TNFα, a prominent pharmacological target in the treatment of rheumatoid arthritis, and TGFα, a key substrate in bone development [35, 36]. The binding capacities of these proteins for sFRP3, as well as the impact of this suppression and the influence of the rare variants of sFRP3, should be addressed *in vitro* and *in vivo*.

Notably, the inhibitory TIMP3-ADAM17 interaction [63] and the inhibitory ADAM17-β_1-integrin complex [64, 65] decompose upon ADAM17 stimulation; however, this decomposition does not occur for ADAM17 and sFRP3 because the interaction was clearly detectable upon activation of ADAM17 by PMA. This difference might point to new mode of regulation. TIMP3 and β_1-integrin prevent the activity of ADAM17 prior to its activation, because the prodomain of the zymogen is already removed in the Golgi apparatus [66], and both interactions are abrogated upon activation of ADAM17. In the case of sFRP3, its interaction with ADAM17 does not diminish upon enzyme activation, supporting its function as a general inhibitor of the protease activity. However, more research is required to confirm this hypothesis and to determine the mechanism by which sFRP3 suppresses the activity of ADAM17, for example, by interacting with the catalytic site or by steric hindrance of proper substrate binding.

In conclusion, the results presented here reveal a novel function of sFRP3 as a suppressor of the important enzyme ADAM17, which acts as a main switch in physiological and pathophysiological situations. This function of sFRP3 can explain how its rare double variant has inferior cartilage protective properties and is associated with arthritis, since it has lost its ADAM17 suppressive ability.

AUTHOR CONTRIBUTION

Experiments and data analysis was performed by Mirja Oldefest, Stefan Düsterhöft, Christine Desel, Christine Fink, Sarah Thysen, Björn Rabe and Inken Lorenzen. Experiments were designed

by Rik Lories, Joachim Grötzinger and Inken Lorenzen. Manuscript was written by Rik Lories, Joachim Grötzinger and Inken Lorenzen. All authors proofread and approved the manuscript.

ACKNOWLEDGMENTS

The authors thank Lea Egli, Britta Hansen, Michelle Horn and Jessica Schneider for their excellent technical assistance, Athena Chalaris for providing AP-proTNFα expression plasmid and Doreen M. Floss for the AP-proTGFα expression plasmid. We are thankful for access to the core facilities of the BiMo/LMB of the CAU and the support by Sebastian Krossa.

FUNDING

This study was supported by the Deutsche Forschungsgemeinschaft (SFB 877, A6 and Z3) and the Excellence Cluster 306 'Inflammation at Interfaces'.

REFERENCES

1 Hoang, B., Moos, M., Jr., Vukicevic, S. and Luyten, F. P. (1996) Primary structure and tissue distribution of FRZB, a novel protein related to Drosophila frizzled, suggest a role in skeletal morphogenesis. J. Biol. Chem. **271**, 26131-26137

2 Hoang, B. H., Thomas, J. T., Abdul-Karim, F. W., Correia, K. M., Conlon, R. A., Luyten, F. P. and Ballock, R. T. (1998) Expression pattern of two Frizzled-related genes, Frzb-1 and Sfrp-1, during mouse embryogenesis suggests a role for modulating action of Wnt family members. Dev. Dyn. **212**, 364-372

3 Enomoto-Iwamoto, M., Kitagaki, J., Koyama, E., Tamamura, Y., Wu, C., Kanatani, N., Koike, T., Okada, H., Komori, T., Yoneda, T., Church, V., Francis-West, P. H., Kurisu, K., Nohno, T., Pacifici, M. and Iwamoto, M. (2002) The Wnt antagonist Frzb-1 regulates chondrocyte maturation and long bone development during limb skeletogenesis. Dev. Biol. **251**, 142-156

4 Tylzanowski, P., Bossuyt, W., Thomas, J. T. and Luyten, F. P. (2004) Characterization of Frzb-Cre transgenic mouse. Genesis. **40**, 200-204

5 Lories, R. J., Peeters, J., Bakker, A., Tylzanowski, P., Derese, I., Schrooten, J., Thomas, J. T. and Luyten, F. P. (2007) Articular cartilage and biomechanical properties of the long bones in Frzb-knockout mice. Arthritis Rheum. **56**, 4095-4103

6 Loughlin, J., Dowling, B., Chapman, K., Marcelline, L., Mustafa, Z., Southam, L., Ferreira, A., Ciesielski, C., Carson, D. A. and Corr, M. (2004) Functional variants within the secreted frizzled-related protein 3 gene are associated with hip osteoarthritis in females. Proc. Natl. Acad. Sci. U S A. **101**, 9757-9762

7 Lories, R. J., Boonen, S., Peeters, J., de Vlam, K. and Luyten, F. P. (2006) Evidence for a differential association of the Arg200Trp single-nucleotide polymorphism in FRZB with hip osteoarthritis and osteoporosis. Rheumatology (Oxford). **45**, 113-114

8 Min, J. L., Meulenbelt, I., Riyazi, N., Kloppenburg, M., Houwing-Duistermaat, J. J., Seymour, A. B., Pols, H. A., van Duijn, C. M. and Slagboom, P. E. (2005) Association of the Frizzled-related protein gene with symptomatic osteoarthritis at multiple sites. Arthritis Rheum. **52**, 1077-1080

9 Lane, N. E., Lian, K., Nevitt, M. C., Zmuda, J. M., Lui, L., Li, J., Wang, J., Fontecha, M., Umblas, N., Rosenbach, M., de Leon, P. and Corr, M. (2006) Frizzled-related protein variants are risk factors for hip osteoarthritis. Arthritis Rheum. **54**, 1246-1254

10 Gordon, A., Southam, L., Loughlin, J., Wilson, A. G., Stockley, I., Hamer, A. J., Eastell, R. and Wilkinson, J. M. (2007) Variation in the secreted frizzled-related protein-3 gene and risk of osteolysis and heterotopic ossification after total hip arthroplasty. J. Orthop. Res. **25**, 1665-1670

11 Shanmugam, K. S., Brenner, H., Hoffmeister, M., Chang-Claude, J. and Burwinkel, B. (2007) The functional genetic variant Arg324Gly of frizzled-related protein is associated with colorectal cancer risk. Carcinogenesis. **28**, 1914-1917
12 Alanazi, M. S., Parine, N. R., Shaik, J. P., Alabdulkarim, H. A., Ajaj, S. A. and Khan, Z. (2013) Association of single nucleotide polymorphisms in Wnt signaling pathway genes with breast cancer in Saudi patients. PLoS One. **8**, e59555
13 Bovolenta, P., Esteve, P., Ruiz, J. M., Cisneros, E. and Lopez-Rios, J. (2008) Beyond Wnt inhibition: new functions of secreted Frizzled-related proteins in development and disease. J Cell Sci. **121**, 737-746
14 Wang, S., Krinks, M., Lin, K., Luyten, F. P. and Moos, M., Jr. (1997) Frzb, a secreted protein expressed in the Spemann organizer, binds and inhibits Wnt-8. Cell. **88**, 757-766
15 Leyns, L., Bouwmeester, T., Kim, S. H., Piccolo, S. and De Robertis, E. M. (1997) Frzb-1 is a secreted antagonist of Wnt signaling expressed in the Spemann organizer. Cell. **88**, 747-756
16 Wang, S., Krinks, M. and Moos, M., Jr. (1997) Frzb-1, an antagonist of Wnt-1 and Wnt-8, does not block signaling by Wnts -3A, -5A, or -11. Biochem. Biophys. Res. Commun. **236**, 502-504
17 Person, A. D., Garriock, R. J., Krieg, P. A., Runyan, R. B. and Klewer, S. E. (2005) Frzb modulates Wnt-9a-mediated beta-catenin signaling during avian atrioventricular cardiac cushion development. Dev. Biol. **278**, 35-48
18 Ekström, E. J., Sherwood, V. and Andersson, T. (2011) Methylation and loss of Secreted Frizzled-Related Protein 3 enhances melanoma cell migration and invasion. PLoS One. **6**, e18674
19 Yamada, A., Iwata, T., Yamato, M., Okano, T. and Izumi, Y. (2013) Diverse functions of secreted frizzled-related proteins in the osteoblastogenesis of human multipotent mesenchymal stromal cells. Biomaterials. **34**, 3270-3278
20 Dann, C. E., Hsieh, J. C., Rattner, A., Sharma, D., Nathans, J. and Leahy, D. J. (2001) Insights into Wnt binding and signalling from the structures of two Frizzled cysteine-rich domains. Nature. **412**, 86-90
21 Lin, K., Wang, S., Julius, M. A., Kitajewski, J., Moos, M., Jr. and Luyten, F. P. (1997) The cysteine-rich frizzled domain of Frzb-1 is required and sufficient for modulation of Wnt signaling. Proc. Natl. Acad. Sci. U S A. **94**, 11196-11200
22 Üren, A., Reichsman, F., Anest, V., Taylor, W. G., Muraiso, K., Bottaro, D. P., Cumberledge, S. and Rubin, J. S. (2000) Secreted frizzled-related protein-1 binds directly to Wingless and is a biphasic modulator of Wnt signaling. J. Biol. Chem. **275**, 4374-4382
23 Bekhouche, M., Kronenberg, D., Vadon-Le Goff, S., Bijakowski, C., Lim, N. H., Font, B., Kessler, E., Colige, A., Nagase, H., Murphy, G., Hulmes, D. J. and Moali, C. (2010) Role of the netrin-like domain of procollagen C-proteinase enhancer-1 in the control of metalloproteinase activity. J. Biol. Chem. **285**, 15950-15959
24 Weiss, T., Ricard-Blum, S., Moschcovich, L., Wineman, E., Mesilaty, S. and Kessler, E. (2010) Binding of procollagen C-proteinase enhancer-1 (PCPE-1) to heparin/heparan sulfate: properties and role in PCPE-1 interaction with cells. J. Biol. Chem. **285**, 33867-33874
25 Bader, H. L., Wang, L. W., Ho, J. C., Tran, T., Holden, P., Fitzgerald, J., Atit, R. P., Reinhardt, D. P. and Apte, S. S. (2012) A disintegrin-like and metalloprotease domain containing thrombospondin type 1 motif-like 5 (ADAMTSL5) is a novel fibrillin-1-, fibrillin-2-, and heparin-binding member of the ADAMTS superfamily containing a netrin-like module. Matrix. Biol. **31**, 398-411
26 Martin-Manso, G., Calzada, M. J., Chuman, Y., Sipes, J. M., Xavier, C. P., Wolf, V., Kuznetsova, S. A., Rubin, J. S. and Roberts, D. D. (2011) sFRP-1 binds via its netrin-related motif to the N-module of thrombospondin-1 and blocks thrombospondin-1 stimulation of MDA-MB-231 breast carcinoma cell adhesion and migration. Arch. Biochem. Biophys. **509**, 147-156

27 Banyai, L. and Patthy, L. (1999) The NTR module: domains of netrins, secreted frizzled related proteins, and type I procollagen C-proteinase enhancer protein are homologous with tissue inhibitors of metalloproteases. Protein Sci. **8**, 1636-1642
28 Lee, M. H., Rapti, M. and Murphy, G. (2005) Total conversion of tissue inhibitor of metalloproteinase (TIMP) for specific metalloproteinase targeting: fine-tuning TIMP-4 for optimal inhibition of tumor necrosis factor-{alpha}-converting enzyme. J. Biol. Chem. **280**, 15967-15975
29 Lee, H. X., Ambrosio, A. L., Reversade, B. and De Robertis, E. M. (2006) Embryonic dorsal-ventral signaling: secreted frizzled-related proteins as inhibitors of tolloid proteinases. Cell. **124**, 147-159
30 Ploper, D., Lee, H. X. and De Robertis, E. M. (2011) Dorsal-ventral patterning: Crescent is a dorsally secreted Frizzled-related protein that competitively inhibits Tolloid proteases. Dev. Biol. **352**, 317-328
31 Muraoka, O., Shimizu, T., Yabe, T., Nojima, H., Bae, Y. K., Hashimoto, H. and Hibi, M. (2006) Sizzled controls dorso-ventral polarity by repressing cleavage of the Chordin protein. Nat. Cell Biol. **8**, 329-338
32 Bijakowski, C., Vadon-Le Goff, S., Delolme, F., Bourhis, J. M., Lecorche, P., Ruggiero, F., Becker-Pauly, C., Yiallouros, I., Stocker, W., Dive, V., Hulmes, D. J. and Moali, C. (2012) Sizzled is unique among secreted frizzled-related proteins for its ability to specifically inhibit bone morphogenetic protein-1 (BMP-1)/tolloid-like proteinases. J. Biol. Chem. **287**, 33581-33593
33 Zi, X., Guo, Y., Simoneau, A. R., Hope, C., Xie, J., Holcombe, R. F. and Hoang, B. H. (2005) Expression of Frzb/secreted Frizzled-related protein 3, a secreted Wnt antagonist, in human androgen-independent prostate cancer PC-3 cells suppresses tumor growth and cellular invasiveness. Cancer Res. **65**, 9762-9770
34 Esteve, P., Sandonis, A., Cardozo, M., Malapeira, J., Ibanez, C., Crespo, I., Marcos, S., Gonzalez-Garcia, S., Toribio, M. L., Arribas, J., Shimono, A., Guerrero, I. and Bovolenta, P. (2011) SFRPs act as negative modulators of ADAM10 to regulate retinal neurogenesis. Nat. Neurosci. **14**, 562-569
35 Saito, K., Horiuchi, K., Kimura, T., Mizuno, S., Yoda, M., Morioka, H., Akiyama, H., Threadgill, D., Okada, Y., Toyama, Y. and Sato, K. (2013) Conditional inactivation of TNFalpha-converting enzyme in chondrocytes results in an elongated growth plate and shorter long bones. PLoS One. **8**, e54853
36 Hall, K. C., Hill, D., Otero, M., Plumb, D. A., Froemel, D., Dragomir, C. L., Maretzky, T., Boskey, A., Crawford, H., Selleri, L., Goldring, M. B. and Blobel, C. P. (2013) ADAM17 controls endochondral ossification by regulating terminal differentiation of chondrocytes. Mol. Cell Biol. **33**, 3077-3090.
37 Black, R. A., Rauch, C. T., Kozlosky, C. J., Peschon, J. J., Slack, J. L., Wolfson, M. F., Castner, B. J., Stocking, K. L., Reddy, P., Srinivasan, S., Nelson, N., Boiani, N., Schooley, K. A., Gerhart, M., Davis, R., Fitzner, J. N., Johnson, R. S., Paxton, R. J., March, C. J. and Cerretti, D. P. (1997) A metalloproteinase disintegrin that releases tumour-necrosis factor-alpha from cells. Nature. **385**, 729-733
38 Moss, M. L., Jin, S. L., Milla, M. E., Bickett, D. M., Burkhart, W., Carter, H. L., Chen, W. J., Clay, W. C., Didsbury, J. R., Hassler, D., Hoffman, C. R., Kost, T. A., Lambert, M. H., Leesnitzer, M. A., McCauley, P., McGeehan, G., Mitchell, J., Moyer, M., Pahel, G., Rocque, W., Overton, L. K., Schoenen, F., Seaton, T., Su, J. L., Becherer, J. D. and al., e. (1997) Cloning of a disintegrin metalloproteinase that processes precursor tumour-necrosis factor-alpha. Nature. **385**, 733-736
39 Scheller, J., Chalaris, A., Garbers, C. and Rose-John, S. (2011) ADAM17: a molecular switch to control inflammation and tissue regeneration. Trends Immunol. **32** 380-387
40 Peschon, J. J., Slack, J. L., Reddy, P., Stocking, K. L., Sunnarborg, S. W., Lee, D. C., Russell, W. E., Castner, B. J., Johnson, R. S., Fitzner, J. N., Boyce, R. W., Nelson, N., Kozlosky, C. J., Wolfson, M. F., Rauch, C. T., Cerretti, D. P., Paxton, R. J., March, C. J. and Black, R. A. (1998) An Essential Role for Ectodomain Shedding in Mammalian Development. Science. **282**, 1281-1284
41 Van Hauwermeiren, F., Vandenbroucke, R. E. and Libert, C. (2011) Treatment of TNF mediated diseases by selective inhibition of soluble TNF or TNFR1. Cytokine Growth Factor Rev. **22**, 311-319
42 Jones, S. A., Scheller, J. and Rose-John, S. (2011) Therapeutic strategies for the clinical blockade of IL-6/gp130 signaling. J. Clin. Invest. **121**, 3375-3383

43 Rose-John, S., Scheller, J., Elson, G. and Jones, S. (2006) Interleukin-6 Biology is Coordinated by Membrane-Bound and Soluble Receptors: Role in Inflammation and Cancer. J. Leuk. Biol. **80**, 227-236
44 Scheller, J., Chalaris, A., Schmidt-Arras, D. and Rose-John, S. (2011) The pro- and anti-inflammatory properties of the cytokine interleukin-6. Biochimica et biophysica acta. **1813**, 878-888
45 Tamura, T., Udagawa, N., Takahashi, N., Miyaura, C., Tanaka, S., Yamada, Y., Koishihara, Y., Ohsugi, Y., Kumaki, K., Taga, T. and et al. (1993) Soluble interleukin-6 receptor triggers osteoclast formation by interleukin 6. Proc. Natl. Acad. Sci. U S A. **90**, 11924-11928
46 Udagawa, N., Takahashi, N., Katagiri, T., Tamura, T., Wada, S., Findlay, D. M., Martin, T. J., Hirota, H., Taga, T., Kishimoto, T. and Suda, T. (1995) Interleukin (IL)-6 induction of osteoclast differentiation depends on IL-6 receptors expressed on osteoblastic cells but not on osteoclast progenitors. J. Exp. Med. **182**, 1461-1468
47 Liu, X., Croker, B. A., Campbell, I. K., Gauci, S. J., Alexander, W. S., Tonkin, B. A., Walsh, N. C., Linossi, E. M., Nicholson, S. E., Lawlor, K. E. and Wicks, I. P. (2014) Key role of suppressor of cytokine signaling 3 in regulating gp130 cytokine-induced signaling and limiting chondrocyte responses during murine inflammatory arthritis. Arthritis Rheumatol. **66**, 2391-2402.
48 Kotake, S., Sato, K., Kim, K. J., Takahashi, N., Udagawa, N., Nakamura, I., Yamaguchi, A., Kishimoto, T., Suda, T. and Kashiwazaki, S. (1996) Interleukin-6 and soluble interleukin-6 receptors in the synovial fluids from rheumatoid arthritis patients are responsible for osteoclast-like cell formation. J. Bone Miner. Res. **11**, 88-95
49 Lorenzen, I., Lokau, J., Düsterhoft, S., Trad, A., Garbers, C., Scheller, J., Rose-John, S. and Grötzinger, J. (2012) The membrane-proximal domain of A Disintegrin and Metalloprotease 17 (ADAM17) is responsible for recognition of the interleukin-6 receptor and interleukin-1 receptor II. FEBS Lett. **586**, 1093-1100
50 Le Gall, S. M., Bobé, P., Reiss, K., Horiuchi, K., Niu, X. D., Lundell, D., Gibb, D. R., Conrad, D., Saftig, P. and Blobel, C. P. (2009) ADAMs 10 and 17 Represent Differentially Regulated Components of a General Shedding Machinery for Membrane Proteins such as TGF{alpha}, L-Selectin and TNF{alpha}. Mol. Biol. Cell. **20**, 1785-1794
51 Garbers, C., Janner, N., Chalaris, A., Moss, M. L., Floss, D. M., Meyer, D., Koch-Nolte, F., Rose-John, S. and Scheller, J. (2011) Species Specificity of ADAM10 and ADAM17 Proteins in Interleukin-6 (IL-6) Trans-signaling and Novel Role of ADAM10 in Inducible IL-6 Receptor Shedding. J. Biol. Chem. **286**, 14804-14811
52 Baran, P., Nitz, R., Grötzinger, J., Scheller, J. and Garbers, C. (2013) Minimal interleukin 6 (IL-6) receptor stalk composition for IL-6 receptor shedding and IL-6 classic signaling. J. Biol. Chem. **288**, 14756-14768
53 Lorenzen, I., Trad, A. and Grötzinger, J. (2011) Multimerisation of A disintegrin and metalloprotease protein-17 (ADAM17) is mediated by its EGF-like domain. Biochem. Biophys. Res. Commun. **415**, 330-336
54 Trad, A., Hedemann, N., Shomali, M., Pawlak, V., Grötzinger, J. and Lorenzen, I. (2011) Development of sandwich ELISA for detection and quantification of human and murine a disintegrin and metalloproteinase17. J. Immunol. Methods. **371**, 91-96
55 Chalaris, A., Rabe, B., Paliga, K., Lange, H., Laskay, T., Fielding, C. A., Jones, S. A., Rose-John, S. and Scheller, J. (2007) Apoptosis is a natural stimulus of IL6R shedding and contributes to the pro-inflammatory trans-signaling function of neutrophils. Blood. **110**, 1748-1755
56 Düsterhoft, S., Höbel, K., Oldefest, M., Lokau, J., Waetzig, G. H., Chalaris, A., Garbers, C., Scheller, J., Rose-John, S., Lorenzen, I. and Grötzinger, J. (2014) A Disintegrin and Metalloprotease 17 Dynamic Interaction Sequence, the Sweet Tooth for the Human Interleukin 6 Receptor. J. Biol. Chem. **289**, 16336-16348

57 Trad, A., Hansen, H. P., Shomali, M., Peipp, M., Klausz, K., Hedemann, N., Yamamoto, K., Mauermann, A., Desel, C., Lorenzen, I., Lemke, H., Rose-John, S. and Grötzinger, J. (2013) ADAM17-overexpressing breast cancer cells selectively targeted by antibody-toxin conjugates. Cancer Immunol. Immunother. **62**, 411-421
58 Yamamoto, K., Trad, A., Baumgart, A., Huske, L., Lorenzen, I., Chalaris, A., Grötzinger, J., Dechow, T., Scheller, J. and Rose-John, S. (2012) A novel bispecific single-chain antibody for ADAM17 and CD3 induces T-cell-mediated lysis of prostate cancer cells. Biochem. J. **445**, 135-144
59 Effenberger, T., von der Heyde, J., Bartsch, K., Garbers, C., Schulze-Osthoff, K., Chalaris, A., Murphy, G., Rose-John, S. and Rabe, B. (2014) Senescence-associated release of transmembrane proteins involves proteolytic processing by ADAM17 and microvesicle shedding. Faseb J. **28**, 4847-4856
60 Amour, A., Slocombe, P. M., Webster, A., Butler, M., Knight, C. G., Smith, B. J., Stephens, P. E., Shelley, C., Hutton, M., Knauper, V., Docherty, A. J. and Murphy, G. (1998) TNF-alpha converting enzyme (TACE) is inhibited by TIMP-3. FEBS Lett. **435**, 39-44
61 Wisniewska, M., Goettig, P., Maskos, K., Belouski, E., Winters, D., Hecht, R., Black, R. and Bode, W. (2008) Structural determinants of the ADAM inhibition by TIMP-3: crystal structure of the TACE-N-TIMP-3 complex. J. Mol. Biol. **381**, 1307-1319
62 Soond, S. M., Everson, B., Riches, D. W. and Murphy, G. (2005) ERK-mediated phosphorylation of Thr735 in TNFalpha-converting enzyme and its potential role in TACE protein trafficking. J. Cell. Sci. **118**, 2371-2380
63 Xu, P., Liu, J., Sakaki-Yumoto, M. and Derynck, R. (2012) TACE Activation by MAPK-Mediated Regulation of Cell Surface Dimerization and TIMP3 Association. Sci. Signal. **5**, ra34
64 Saha, A., Backert, S., Hammond, C. E., Gooz, M. and Smolka, A. J. (2010) Helicobacter pylori CagL activates ADAM17 to induce repression of the gastric H, K-ATPase alpha subunit. Gastroenterology. **139**, 239-248
65 Göoz, P., Dang, Y., Higashiyama, S., Twal, W. O., Haycraft, C. J. and Gooz, M. (2012) A disintegrin and metalloenzyme (ADAM) 17 activation is regulated by alpha5beta1 integrin in kidney mesangial cells. PLoS One. **7**, e33350
66 Endres, K., Anders, A., Kojro, E., Gilbert, S., Fahrenholz, F. and Postina, R. (2003) Tumor necrosis factor-alpha converting enzyme is processed by proprotein-convertases to its mature form which is degraded upon phorbol ester stimulation. Eur. J. Biochem. **270**, 2386-2393

FIGURE LEGENDS

Figure 1: ADAM17-mediated IL-6R shedding is suppressed by the common variant of sFRP3 but not its rare double variant. (**A**) HEK293T cells were transiently co-transfected with AP-tagged IL-6R and a control plasmid or a plasmid expressing sFRP3, sFRP3 R324G, or sFRP3 R200W R324G. One day later, ADAM17 activity was stimulated by the addition of 100 nM PMA for 30 minutes. As controls, cells were either untreated (DMSO) or stimulated by PMA in the presence of the metalloprotease inhibitor marimastat (Ma). After the supernatants and lysates were harvested, the AP activities were measured and the relative shedding activities were calculated from the ratio between the supernatant and lysate, as described previously [49, 51, 52]. The shedding activities were first normalized to the PMA- and marimastat-treated samples; thereby their values were set to one. Then the relative AP activities of the PMA-treated control samples were set to 100 %. The mean, standard deviations and significance (Student's t-test) of six independent experiments were calculated. ***$P < 0.001$, which was considered significant. (**B**) To confirm that the observed effect of sFRP3 on IL-6R shedding activity was not due to

variations in the expression levels of the AP-tagged IL-6R or sFRP3 variants, Western blot analyses of the cell lysates were performed. sFRP3 and its variants contained an N-terminal PC-tag, which was introduced between the signal peptide and the CRD, and was used for detection by a murine anti-PC mAb (HPC4). AP-tagged IL-6R was detected using a mAb against human IL-6R [55]. β-actin was used as a loading control. (**C**) Suppression of ADAM17 activity by sFRP3 was not abrogated by the single R200W variant. The experiments were performed as described in (A). (**D**) Correct expression of the transfected constructs within the experiment shown in (C) was confirmed by Western blotting, as described in (B). (**E**) ADAM17 activity assay performed as described for (A), with the exceptions that cells were transfected solely with AP-tagged IL-6R and incubated with conditioned medium from HEK293T cells, containing the indicated proteins, during PMA stimulation. As a control, conditioned medium from HEK293T cells expressing eGFP was used. The mean, standard deviation, and significance (Student's t-test) of five independent experiments were calculated. $^{**}P < 0.01$ and $^{*}P < 0.05$, both of which were considered significant. (**F**) To confirm that the differences in the ADAM17 activities were not due to differences in the expression levels of the sFRP3 constructs, conditioned media (supernatants) and the corresponding cell lysates were analysed by Western blotting before use in shedding assays (E). (**G**) sFRP3 suppressed ADAM17-mediated shedding of extracellular AP-tagged proTNFα and proTGFα. These experiments were performed as described in (A), with the exception that ADAM17 activity was stimulated for 1 h in the case of AP-tagged proTNFα. (**H**) Equal expression levels of overexpressed proteins were confirmed by Western blotting. The C-terminal AP-tagged proTNFα was detected by its myc-tag. N-terminal AP-tagged proTGFα was detected using an antibody recognizing the AP-tag.

Figure 2: Suppression of ADAM17 by sFRP3 is independent of the Wnt signalling pathway. (**A**) The first row of the Wnt Signaling Phospho Antibody Microarray, which was probed with lysates of HEK293T cells stimulated for 5 minutes with PMA in the presence or absence of sFRP3. (**B–E**) The ratios of the signal intensities of sFRP3-treated and untreated (eGFP) samples. The graphs show typical examples of signalling molecules involved in the canonical Wnt signalling pathway (**B**), the planar cell polarity Wnt signalling pathway (**C**), and the calcium Wnt signalling pathway (**D**), as well as other molecules (**E**). The white bars represent the ratios of protein levels, independent of their phosphorylation, and the grey bars represent the ratios of specific phosphorylation sites. The microarray revealed no significant differences between the phosphorylation statuses of molecules in the sFRP3-treated and untreated cells. No changes in the protein expression levels were expected as cells were only stimulated for 5 minutes; hence variations in the ratios up to 0.3 were part of the normal variation within the assay. No consistent tendencies were detectable for a single Wnt pathway; therefore, the assay was only performed once and no error bars could be shown.

Figure 3: sFRP3 interacts with ADAM17. (**A**) N-terminal PC-tagged sFRP3 was co-immunoprecipitated with C-terminal HA-tagged ADAM17. Both proteins were co-expressed in HEK293T cells. HA-tagged ADAM17 was immunoprecipitated from one half of the cell lysate. The second half of the lysate was used as a control and was treated similarly, but no Ab was added. (**B**) Co-immunoprecipitation (IP) of endogenously expressed proteins. ADAM17 was precipitated from lysates of HEK293T cells using the A300E mAb. The pull-down was analysed by

Western blotting using A300D [54] and a rabbit H170 Ab to detect ADAM17 and sFRP3, respectively. (**C**) Confirmation of ADAM17 knock-down in PC3 cells by Western blotting. Expression of ADAM17 was analysed in HEK293T cells as well as stably transfected PC3 cell lines expressing a scrambled shRNA or an ADAM17-specific shRNA [59]. The levels of the proform of ADAM17, containing the prodomain, as well as mature ADAM17, which lacks the prodomain, were lower in the sample from the ADAM17-specific shRNA-transfected PC3 cells than the sample from the scrambled shRNA-transfected cells. β-actin was detected as a loading control. (**D**) Cell surface expression of ADAM17 was lower in PC3 cells transfected with shRNA targeting the protease (blue) than control cells (light green), both prior to and after 5 minutes of PMA stimulation (purple and dark green, respectively). (**E**) Increased sFRP3 cell surface localization due to the cell surface presence of ADAM17. The presence of sFRP3 on the cell surface was dependent on ADAM17. Flow cytometric measurements revealed an increase in sFRP3 cell surface staining in ADAM17-expressing PC3 cells (green), compared with ADAM17 knock-down PC3 cells (red).

Figure 4: Figure 4: Cell surface interaction of sFRP3 and ADAM17. (**A–D**). Co-immunostaining of sFRP3 and ADAM17 on the surface of untreated cells. (**E–H**) Co-immunostaining of sFRP3 and ADAM17 on the surface of cells stimulated for 5 minutes with PMA. (**A, E**) sFRP3 and (**B, F**) ADAM17 staining, together with DAPI-stained nuclei. (**C, G**) Merged images were overlaid onto the differential interference images. The red boxes show magnifications of the white boxes within the overlays. (**D, H**) The colocalization modus of *Olympus Fluoview FV 1000* indicated no colocalization of ADAM17 and sFRP3 in untreated cells, but 10 % colocalization in cells treated for 5 minutes with PMA prior to staining. In both experiments, non-permeabilized HEK293T cells were stained with a rabbit polyclonal anti-sFRP3 Ab (H170) and a murine anti-ADAM17 A300E mAb, and the nuclei were stained with DAPI. Scale bars, 10 µm. (**I**) HEK293T cells showed an increased ADAM17 presence after stimulation with PMA as shown by flow cytometry. After 5 minutes of PMA treatment, the amount of ADAM17 was increased. (**J**) Cell surface biotinylation of ADAM17. Cell surface proteins of HEK293T cells, which were untreated or treated for 30 minutes with PMA, were biotinylated. The biotinylated proteins were precipitated using streptavidin beads and the presence of ADAM17 was determined by Western blotting. As a control for intact cells, Western blotting was performed to detect β-actin. (**K**) sFRP3 and ADAM17 interaction on the surface of HEK293T cells was confirmed by a proximity ligation assay (Duolink in Situ® Assay; Sigma-Aldrich) using a rabbit anti-sFRP3 Ab and a murine anti-ADAM17 mAb. The cells were stained with primary and secondary Abs, directed against murine or rabbit heavy chains. The secondary Abs were conjugated with special oligonucleotides, which, in the case of close proximity of both target proteins, hybridized and formed a cyclic DNA double helix. In the final step, a rolling cycle amplification induced by exogenous polymerase occurred. Together with the addition of fluorescent labeled oligonucleotides that hybridize to the rolling cycle amplification product, an amplified signal of the interaction could be detected. Green spots appeared only if the target proteins were in close proximity. (**L**) In the control sample, only one primary Ab directed against ADAM17 was used. All other steps were performed as described for (K). For the control, only background and non-specific amplified DNA should be detected. (**M**) Surface plasmon resonance measurements confirming low affinity binding between ADAM17 and sFRP3. The extracellular part of mature ADAM17 was immobilized and

the binding capacity of sFRP3 in PBS was analysed. (**N**) Flow cytometric analysis of rare sFRP3 variants, performed as described for the common variant (Figure 3E). Analysis of the R200W and R324G single variants and the R200W R324G double variant revealed that only the latter failed to interact with ADAM17 on the surface of PC3 cells. (**O, P**) Western blot analysis demonstrating comparable expression of the rare variants of sFRP3 in PC3 cells relative to the common variant. Cell lysates left over from the flow cytometry analysis (N) were analysed to determine the expression of PC-tagged sFRP3 variants and β-actin. The non-cut image of Western blot (O) is shown in Supplementary Figure S1.

Figure 5: Cell surface interaction of sFRP3 and IL-6R. (**A**) Co-immunoprecipitation analyses of sFRP3 and IL-6R. PC-tagged sFRP3 and IL-6R were co-transfected into HEK293T cells. After cell lysis, sFRP3 was immunoprecipitated using an anti-HPC4 mAb, and co-precipitated IL-6R was detected by Western blotting. (**B**) Reverse experiment of that described in (A). IL-6R was precipitated using mAb 4-11 [55] and sFRP3 was detected by Western blotting. (**C**) Flow cytometric analyses of IL-6R cell surface expression. Isotope control (grey), cells transfected with IL-6R and pcDNA3.1 (blue), and cells transfected with sFRP3 and IL-6R (red). (**D**) Analysis of the sFRP3 cell surface presence by flow cytometry using an anti-HPC4 mAb for detection. Isotope control (grey), cells transfected with sFRP3 and pcDNA3.1 (blue), and cells transfected with sFRP3 and IL-6R (red). (**E, F**) The rare double variant of sFRP3 interacted with IL-6R on the cell surface. Experiments were performed as described in (C, D). (**G**) Proximity ligation assay to confirm the interaction of sFRP3 with IL-6R. A murine mAb A300E and a rabbit anti-sFRP3 Ab were used as primary Abs. (**H**) The control sample of (G); the preparation was treated in the same way, with the exception that mAb A300E was the only primary Ab used.

FIGURES

Figure 1

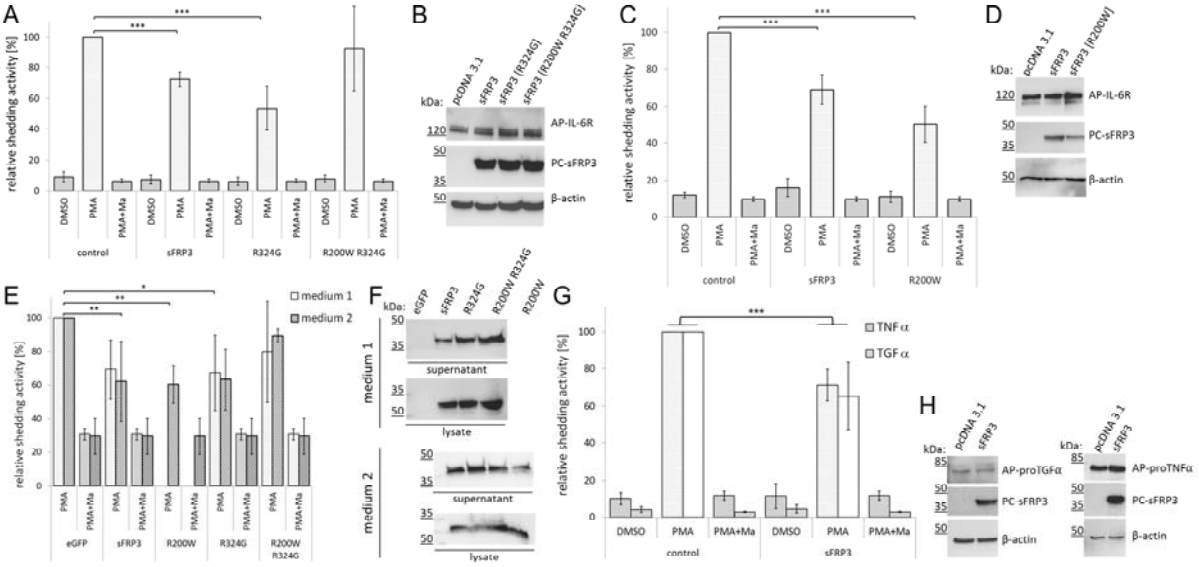

Figure 2

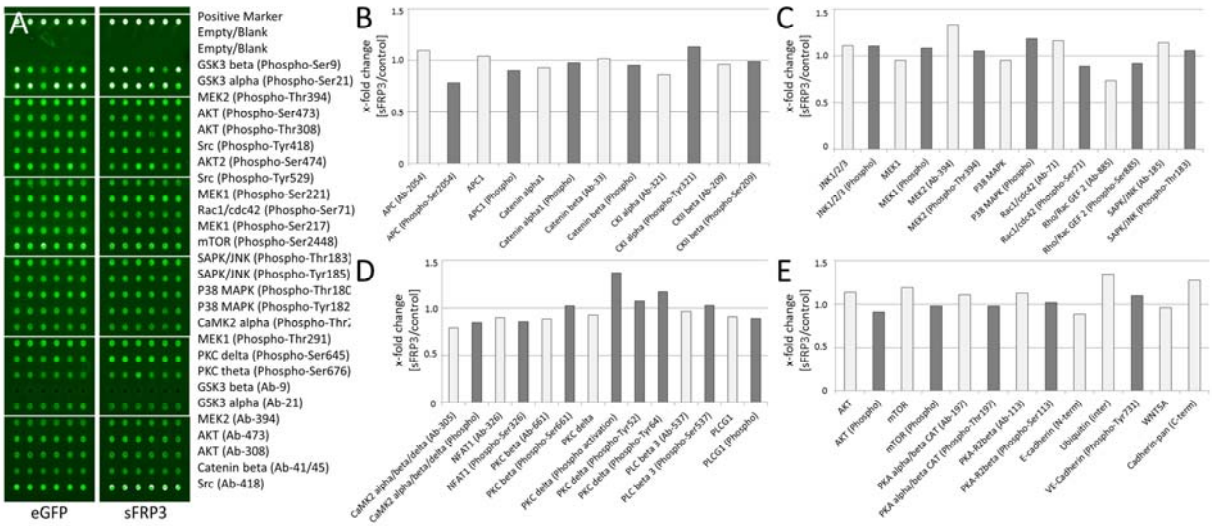

Figure 3

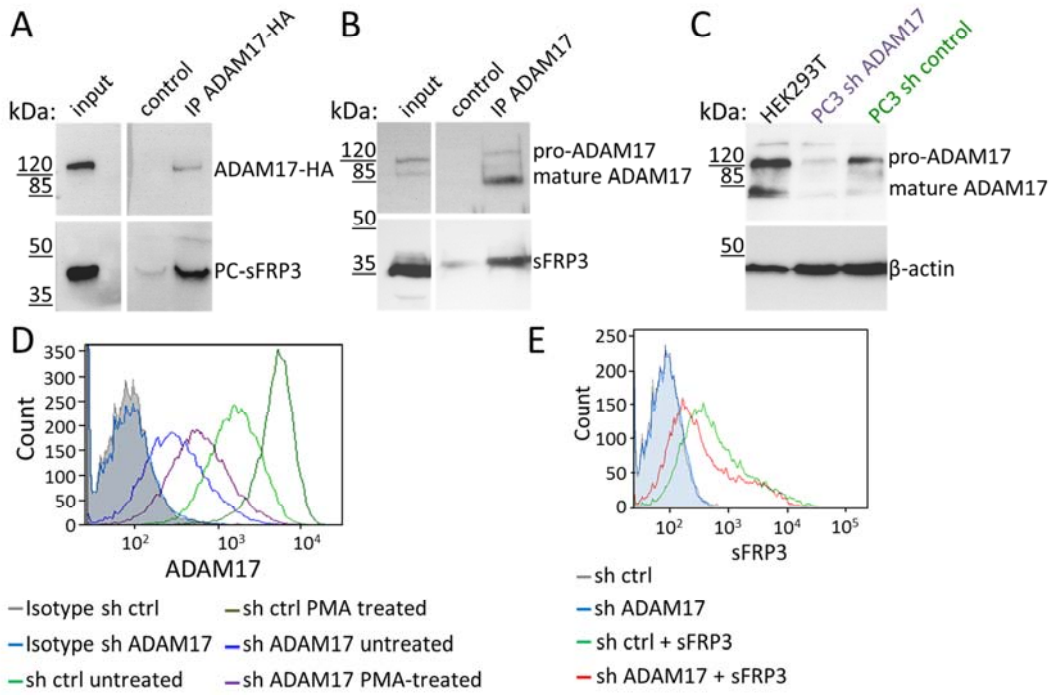

Figure 4

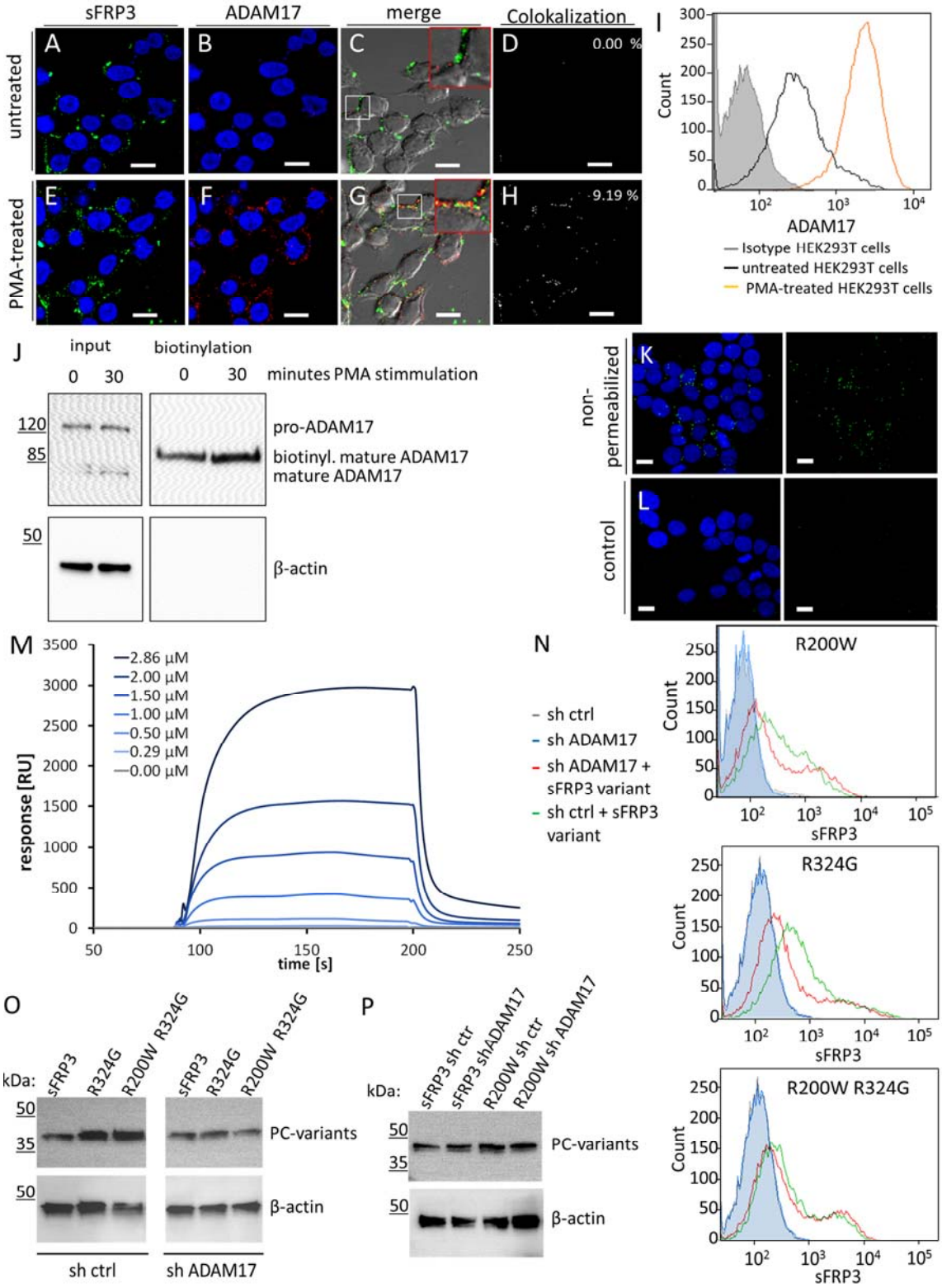
sFRP3
ADAM17
merge
Colokalization
untreated
PMA-treated
A
B
C
D
0.00 %
E
F
G
H
9.19 %
I
Count
ADAM17
Isotype HEK293T cells
untreated HEK293T cells
PMA-treated HEK293T cells
J
input
biotinylation
0 30 0 30 minutes PMA stimmulation
120
85
pro-ADAM17
biotinyl. mature ADAM17
mature ADAM17
50
β-actin
non-permeabilized
control
K
L
M
response [RU]
time [s]
2.86 µM
2.00 µM
1.50 µM
1.00 µM
0.50 µM
0.29 µM
0.00 µM
N
sh ctrl
sh ADAM17
sh ADAM17 + sFRP3 variant
sh ctrl + sFRP3 variant
R200W
R324G
R200W R324G
sFRP3
O
kDa:
sFRP3
R324G
R200W R324G
50
35
PC-variants
β-actin
sh ctrl
sh ADAM17
P
sFRP3 sh ctr
sFRP3 shADAM17
R200W sh ctr
R200W sh ADAM17

Figure 5

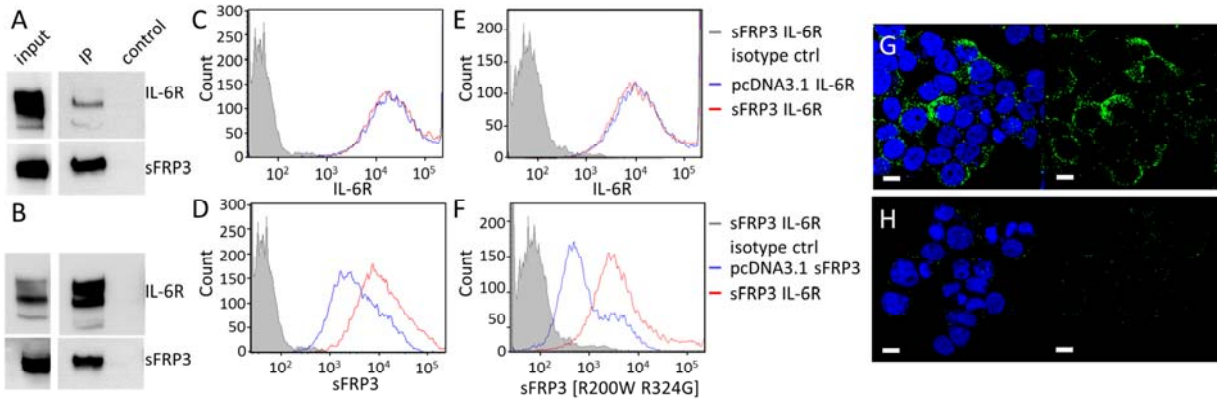
A
input
IP
control
IL-6R
sFRP3
B
IL-6R
sFRP3
C
Count
IL-6R
D
Count
sFRP3
E
Count
IL-6R
F
Count
sFRP3 [R200W R324G]
sFRP3 IL-6R
isotype ctrl
pcDNA3.1 IL-6R
sFRP3 IL-6R
sFRP3 IL-6R
isotype ctrl
pcDNA3.1 sFRP3
sFRP3 IL-6R
G
H